

Toshio Iwasaki,^{a*} Asako
Kounosu,^a Daijiro Ohmori^b and
Takashi Kumasaka^{c*}

^aDepartment of Biochemistry and Molecular
Biology, Nippon Medical School, Sendagi,
Bunkyo-ku, Tokyo 113-8602, Japan,

^bDepartment of Chemistry, Juntendo University,
Inba, Chiba 270-1695, Japan, and ^cDepartment
of Life Science, Tokyo Institute of Technology,
Nagatsuta, Midori-ku, Yokohama 226-8501,
Japan

Correspondence e-mail: tiwasaki@nms.ac.jp,
tkumasak@bio.titech.ac.jp

Received 10 August 2006

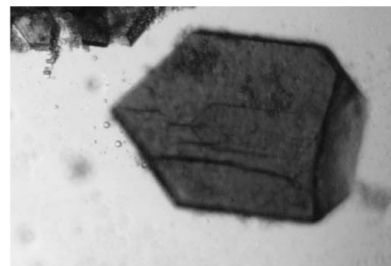
Accepted 28 August 2006

Crystallization and preliminary X-ray diffraction studies of a hyperthermophilic Rieske protein variant (SDX-triple) with an engineered rubredoxin-like mononuclear iron site

In place of the Rieske [2Fe–2S] cluster, an archetypal mononuclear iron site has rationally been designed into a hyperthermophilic archaeal Rieske [2Fe–2S] protein (sulredoxin) from *Sulfolobus tokodaii* by three residue replacements with reference to the *Pyrococcus furiosus* rubredoxin sequence. The resulting sulredoxin variant, SDX-triple (H44I/A45C/H64C), has been purified and crystallized by the hanging-drop vapour-diffusion method using 65%(v/v) 2-methyl-2,4-pentanediol, 0.025 M citric acid and 0.075 M sodium acetate trihydrate pH 4.3. The crystals diffract to 1.63 Å resolution and belong to the triclinic space group *P*1, with unit-cell parameters $a = 43.56$, $b = 76.54$, $c = 80.28$ Å, $\alpha = 88.12$, $\beta = 78.82$, $\gamma = 73.46^\circ$. The asymmetric unit contains eight protein molecules.

1. Introduction

The utilization of a limited number of protein scaffolds produces proteins with different types of active sites for various biological catalysis, molecular recognition and metabolic requirements (DeGrado *et al.*, 1999; Lu *et al.*, 2001). Recent site-directed mutagenesis studies have indicated the importance of types and spacing of terminal ligands in the *in vivo* cluster recognition/insertion/assembly in metallosulfur protein scaffolds. Replacement of Cys42 by alanine allows the (unexpected) incorporation of an oxidized [2Fe–2S] cluster into the *Clostridium pasteurianum* rubredoxin (Rd) polypeptide chain, which normally accommodates a mononuclear Fe(Cys)₄ site (Meyer *et al.*, 1997). Conversely, by mimicking the mononuclear iron site in the *Pyrococcus furiosus* Rd involved in the molecular oxygen-scavenging system (Day *et al.*, 1992; Jenney *et al.*, 1999; Adams *et al.*, 2002), replacement of three residues (His44, Lys45 and His64) in the archaeal Rieske-type [2Fe–2S] ferredoxin (ARF) from *Sulfolobus solfataricus* P-1 by cysteines and isoleucine (ARF-triple; H44I/K45C/H64C) resulted in an Rd-type mononuclear Fe(Cys)₄ site in the Rieske-type protein scaffold (Kounosu *et al.*, 2004; Iwasaki *et al.*, 2005; Fig. 1). A deeper understanding of the metal-binding site design and evolutionary divergency from the same protein template to



© 2006 International Union of Crystallography
All rights reserved

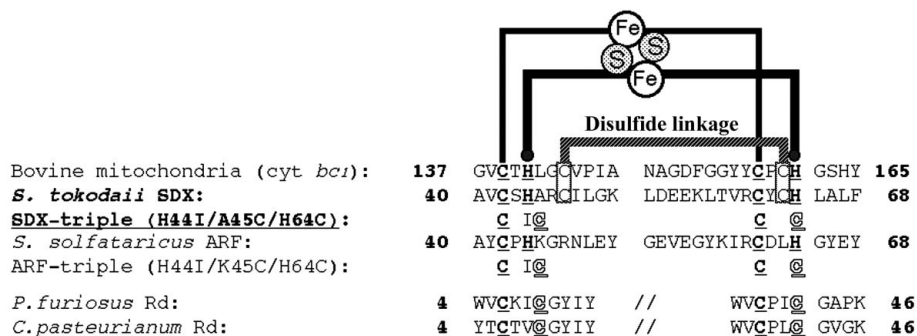


Figure 1

Multiple sequence alignment of the metal-binding sites of selected Rieske proteins and Rds. The cluster-binding motif of *S. tokodaii* SDX is characteristic of the high-potential Rieske protein family and has two conserved cysteine residues that serve as the solvent-exposed disulfide linkage (boxed; Kounosu *et al.*, 2004; Iwasaki *et al.*, 2005). Accession Nos.: bovine mitochondrial cytochrome *bc*₁-associated Rieske protein fragment, P13272; *S. tokodaii* SDX, AB023295; *S. solfataricus* ARF (hypothetical ORF c06009), CAA669492, AB047031; *P. furiosus* Rd, P24297; *C. pasteurianum* Rd, P00268. The metal-binding motifs are underlined.

promote new and specific functionalities would require a knowledge of structural information at atomic resolution, but no suitable crystals of ARF-triple have been produced.

Proteins containing Rieske-type [2Fe-2S] clusters play important electron-transfer roles in various key pathways such as aerobic respiration, photosynthesis and biodegradation of various alkene and aromatic compounds (Mason & Cammack, 1992; Trumpower & Gennis, 1994; Link, 1999; Berry *et al.*, 2000; Crofts, 2004). X-ray crystal structures of several Rieske-type protein domains from various sources (Iwata *et al.*, 1996; Carrell *et al.*, 1997; Kauppi *et al.*, 1998; Colbert *et al.*, 2000; Bönisch *et al.*, 2002; Hunsicker-Wang *et al.*, 2003; PDB codes 1rie, 1rfs, 1ndo, 1fqt, 1jml and 1nyk, respectively) have established that the Rieske-type cluster has an asymmetric [2Fe-2S] core, with the S^γ atom of each of the two cysteine residues coordinated to one iron site and the N^δ atom of each of the two histidine residues coordinated to the other iron site. Among the Rieske-type [2Fe-2S] proteins characterized so far, archaeal sul-redoxin (SDX) from the hyperthermoacidophile *S. tokodaii* strain 7 (DDBJ-EMBL-GenBank accession No. AB023295) is the closest homologue of the *S. solfataricus* ARF (Kounosu *et al.*, 2004; Iwasaki *et al.*, 2004). This 12 kDa protein is unusual in that it is also weakly homologous to the extrinsic cluster-binding domain of cytochrome *bc*-associated Rieske proteins with a solvent-exposed consensus disulfide linkage, despite the inherent absence of the transmembrane domain (Iwasaki *et al.*, 1995; Kounosu *et al.*, 2004; Iwasaki *et al.*, 2004, 2006). Recombinant SDX has been overproduced in *Escherichia coli* and crystallized (Uchiyama *et al.*, 2004) and its crystal structure was recently solved at 2.0 Å resolution using iron multiple-wavelength anomalous diffraction phasing (in preparation). Here, we report the rational design of the Rd-type mononuclear iron site (in place of the Rieske [2Fe-2S] centre) by introduction of three-residue substitutions (H44I/A45C/H64C) into the *S. tokodaii* SDX sequence (Fig. 1) and present the crystallization of the resultant SDX variant (SDX-triple) in a form suitable for high-resolution X-ray studies and preliminary X-ray data analysis.

2. Methods and results

2.1. Protein preparation and characterization

The *sdx* gene coding for the archaeal sul-redoxin (DDBJ-EMBL-GenBank accession No. AB023295) of *S. tokodaii* strain 7 (JCM 10545^T; formerly *Sulfolobus* sp. strain 7; Suzuki *et al.*, 2002) has been cloned and sequenced (Kounosu *et al.*, 2004; Iwasaki *et al.*, 2004). Site-directed mutagenesis was performed by the polymerase chain reaction (PCR) mutagenesis technique with a Quick Change Site-directed Mutagenesis Kit (Stratagene) using a pET28aSDX vector harbouring the *sdx* gene (Kounosu *et al.*, 2004; Iwasaki *et al.*, 2004) as a long template. For the SDX-triple mutant (replacements of His44 by isoleucine, Ala45 by cysteine and His64 by cysteine; H44I/A45C/H64C; Fig. 1), PCR mutagenesis was carried out in a stepwise manner with the following PCR primers: 5'-GAT GCT GTA TGT TCA ATC TGT AGG TGT ATT TTA GG-3' and 5'-CCT AAA ATA CAC CTA CAG ATT GAA CAT ACA GCA TC-3' for H44I/A45C and 5'-GTT AGA TGT TAC TGC TGT CTA GCA TTA TTT GAT CTA AGG-3' and 5'-CCT TAG ATC AAA TAA TGC TAG ACA GCA GTA ACA TCT AAC-3' for H64C. Each amplified PCR product was individually treated with *DpnI* and transformed into *E. coli* HB101 competent cells. In each case, the nucleotide sequences of the resultant vectors were confirmed for both strands with an automatic DNA sequencer, ABI PRISM 310 Genetic Analyzer (PE Biosystems), before subjecting them to the second round of PCR mutagenesis.

The resultant pET28aSDXtriple vector harbouring the *sdx* mutant was transformed into the host strain, *E. coli* BL21-CodonPlus(DE3)-RIL strain (Stratagene). The transformants were grown overnight at 298 K in Luria-Bertani medium containing 50 µg ml⁻¹ kanamycin and 0.2 mM FeCl₃ to enrich the iron content of the SDX-triple variant and the recombinant holoprotein was overproduced with 1 mM isopropyl β-D-thiogalactopyranoside for 24 h at 298 K. The cells were pelleted by centrifugation and the recombinant SDX-triple variant having a hexahistidine-tag at the N-terminus was purified as reported previously for the wild-type protein (Kounosu *et al.*, 2004; Iwasaki *et al.*, 2004). These mutations resulted in heterologous overproduction of a ruby-coloured recombinant protein in *E. coli*, in contrast to the dark reddish purple colour of the wild-type protein (Fig. 2*a*). After proteolytic removal of the hexahistidine tag from the purified SDX-triple for 16–22 h at 297 K using a Thrombin Cleavage Capture Kit (Novagen) according to the manufacturer's instructions, the sample

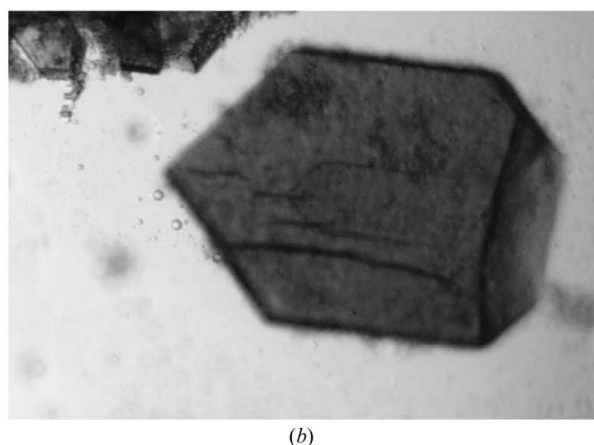
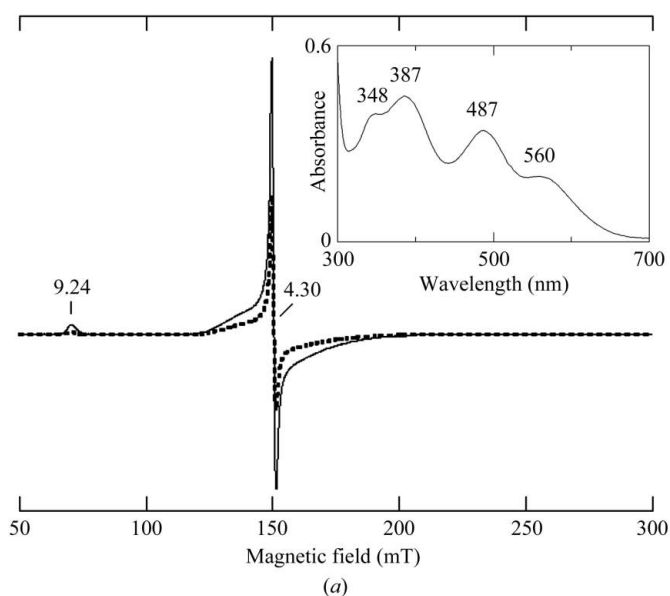


Figure 2
(*a*) X-band EPR spectra at 4.2 K (solid lines) and 12.1 K (dashed lines) of the oxidized SDX-triple (H44I/A45C/H64C) variant, measured using a JES-FA300 spectrometer equipped with an ES-CT470 Heli-Tran cryostat system and a Scientific Instruments digital temperature indicator/controller Model 9650 with the following settings: microwave power, 1.0 mW; modulation amplitude, 0.2 mT. The *g* values are indicated in the figure. The inset shows the visible–near-UV absorption spectrum of the purified SDX-triple variant recorded at room temperature with a Beckman DU-7400 spectrophotometer. (*b*) Typical crystals of the SDX-triple variant. The maximum dimensions of the triclinic crystals are approximately 0.2 × 0.2 × 0.05 mm.

Table 1

Data-processing statistics.

Values in parentheses are for the outer shell.

Space group	<i>P</i> 1
Unit-cell parameters (Å, °)	<i>a</i> = 43.56, <i>b</i> = 76.54, <i>c</i> = 80.28, $\alpha = 88.12$, $\beta = 78.82$, $\gamma = 73.46$
Resolution range (Å)	50.00–1.63 (1.69–1.63)
No. of measured reflections	223712
No. of unique reflections	113049
Completeness (%)	93.4 (74.1)
$R_{\text{merge}}^{\dagger}$ (%)	3.0 (14.1)
$\langle I/\sigma(I) \rangle$	18.9

$\dagger R_{\text{merge}} = \frac{\sum_{hkl} \sum_j |I_j(hkl) - \langle I(hkl) \rangle|}{\sum_{hkl} \sum_j I_j(hkl)}$, where $I_j(hkl)$ and $\langle I(hkl) \rangle$ are the intensity of measurement *j* and the mean intensity for the reflection with indices *hkl*, respectively.

was further purified by gel-filtration chromatography (Sephadex G-50; Amersham Pharmacia Biotech) eluted with 20 mM Tris-HCl, 350 mM NaCl pH 7.5 and concentrated with a Centrprep-10 apparatus (Amicon) to ~3.5 mM (based on the iron content determined by atomic absorption spectroscopy; Hitachi Z-8100) and stored frozen (193 K) until use.

The visible absorption and electron paramagnetic resonance (EPR) spectra of the purified SDX-triple variant clearly showed the presence of a high-spin ferric iron site (Fig. 2*a*). It displays a resonance at $g = 9.24$ associated with one principal direction of the lowest Kramers doublet ($\pm 1/2$ or $\pm 5/2$) at 4.2 K and a number of features in the $g \simeq 3.8$ –4.7 range associated with the three principal directions of the $\pm 3/2$ doublet. These features are very similar to those reported for archaeal and bacterial Rds (Hagen, 1992; Xiao *et al.*, 1998).

2.2. Crystallization

Preliminary screening was by standard hanging-drop vapour diffusion in Linbro plates at 277–293 K with 0.45–0.48 ml reservoirs of commercially available sparse-matrix screening kits [Hampton Research Crystal Screen kits I and II and Grid Screen 2-methyl-2,4-pentanediol (MPD) and Emerald BioStructures kits Cryo I and II]. Two well shaped crystal forms were obtained under conditions where wild-type SDX crystals (Uchiyama *et al.*, 2004) did not grow, but one of them [obtained with 35% (*v/v*) *t*-butanol as a precipitant] gave diffuse diffraction spots and had extremely high mosaicity (data not shown). Optimized crystals were obtained under aerobic conditions in 4–6 d at 293 K by combining 1.0–2.5 μ l protein solution with 0.5–1.0 μ l reservoir solution containing 65% (*v/v*) MPD, 0.025 *M* citric acid and 0.075 *M* sodium acetate trihydrate pH 4.3 and pretreating the resultant hanging droplets in Linbro plates for 5–16 h at 277 K. The crystals grew to maximum dimensions of 0.2 \times 0.2 \times 0.05 mm in about one month (Fig. 2*b*). The crystals could be flash-cooled successfully in liquid nitrogen without being transferred to a cryoprotectant solution.

2.3. Crystallographic data collection and processing

X-ray diffraction data of the SDX-triple variant were collected from flash-frozen crystals using a Rigaku/MSJ Jupiter 210 CCD detector installed on the BL26B1 beamline at SPring-8, Japan. Data collection was performed with a total oscillation range of 200° and a step size of 1.0° with exposure times of 20 s (total exposure time 67 min). Of the two well shaped crystal forms obtained in the initial screening, the triclinic crystals (Fig. 2*b*) were found to diffract to 1.63 Å resolution and to belong to space group *P*1, with unit-cell

parameters $a = 43.56$, $b = 76.54$, $c = 80.28$ Å, $\alpha = 88.12$, $\beta = 78.82$, $\gamma = 73.46$ ° (Table 1). Assuming eight SDX-triple molecules per asymmetric unit, the Matthews coefficient is 2.4 Å³ Da⁻¹, corresponding to a solvent content of 49% (Matthews, 1968).

Phase determination was successfully carried out by the molecular-replacement method from the atomic model of the wild-type SDX using the program *MOLREP* (Vagin & Teplyakov, 1997; Table 1). Construction, revision and analysis of atomic models using the SDX-triple sequence are currently in progress.

We thank Drs M. Yamamoto and G. Ueno for data collection on the BL26B1 beamline at SPring-8. This work was supported in part by The Japanese MEXT Grants-in-Aid 15770088 and 18608004 to TI and a grant from The National Project on Protein Structural and Functional Analyses (Priority Research Program, Protein 3000 Project) to TK.

References

- Adams, M. W. W., Jenney, F. E. Jr, Clay, M. D. & Johnson, M. K. (2002). *J. Biol. Inorg. Chem.* **7**, 647–652.
- Berry, E. A., Guergova-Kuras, M., Huang, L.-S. & Crofts, A. R. (2000). *Annu. Rev. Biochem.* **69**, 1005–1075.
- Bönisch, H., Schmidt, C. L., Schäfer, G. & Ladenstein, R. (2002). *J. Mol. Biol.* **319**, 791–805.
- Carrell, C. J., Zhang, H., Cramer, W. A. & Smith, J. L. (1997). *Structure*, **5**, 1613–1625.
- Colbert, C. L., Couture, M. M.-J., Eltis, L. D. & Bolin, J. (2000). *Structure*, **8**, 1267–1278.
- Crofts, A. R. (2004). *Annu. Rev. Physiol.* **66**, 689–733.
- Day, M. W., Hsu, B. T., Joshua-Tor, L., Park, J. B., Zhou, Z. H., Adams, M. W. W. & Rees, D. C. (1992). *Protein Sci.* **1**, 1494–1507.
- DeGrado, W. F., Summa, C. M., Pavone, V., Nastro, F. & Lombardi, A. (1999). *Annu. Rev. Biochem.* **68**, 779–819.
- Hagen, W. R. (1992). *Adv. Inorg. Chem.* **38**, 165–222.
- Hunsicker-Wang, L. M., Heine, A., Chen, Y., Luna, E. P., Todaro, T., Zhang, Y. M., Williams, P. A., McRee, D. E., Hirst, J., Stout, C. D. & Fee, J. A. (2003). *Biochemistry*, **42**, 7303–7317.
- Iwasaki, T., Isogai, T., Iizuka, T. & Oshima, T. (1995). *J. Bacteriol.* **177**, 2576–2582.
- Iwasaki, T., Kounosu, A., Kolling, D. R. J., Crofts, A. R., Dikanov, S. A., Jin, A., Imai, T. & Urushiyama, A. (2004). *J. Am. Chem. Soc.* **126**, 4788–4789.
- Iwasaki, T., Kounosu, A., Samoilova, R. I. & Dikanov, S. A. (2006). *J. Am. Chem. Soc.* **128**, 2170–2171.
- Iwasaki, T., Kounosu, A., Tao, Y., Li, Z., Shokes, J. E., Cospers, N. J., Imai, T., Urushiyama, A. & Scott, R. A. (2005). *J. Biol. Chem.* **280**, 9129–9134.
- Iwata, S., Saynovits, M., Link, T. A. & Michel, H. (1996). *Structure*, **4**, 567–579.
- Jenney, F. E. Jr, Verhagen, M. F., Cui, X. & Adams, M. W. W. (1999). *Science*, **286**, 306–309.
- Kauppi, B., Lee, K., Carredano, E., Parales, R. E., Gibson, D. T., Eklund, H. & Ramaswamy, S. (1998). *Structure*, **6**, 571–586.
- Kounosu, A., Li, Z., Cospers, N. J., Shokes, J. E., Scott, R. A., Imai, T., Urushiyama, A. & Iwasaki, T. (2004). *J. Biol. Chem.* **279**, 12519–12528.
- Link, T. A. (1999). *Adv. Inorg. Chem.* **47**, 83–157.
- Lu, Y., Berry, S. M. & Pfister, T. D. (2001). *Chem. Rev.* **101**, 3047–3080.
- Mason, J. R. & Cammack, R. (1992). *Annu. Rev. Microbiol.* **46**, 277–305.
- Matthews, B. W. (1968). *J. Mol. Biol.* **33**, 491–497.
- Meyer, J., Gagnon, J., Gaillard, J., Lutz, M., Achim, C., Münck, E., Pétilot, Y., Colangelo, C. M. & Scott, R. A. (1997). *Biochemistry*, **36**, 13374–13380.
- Suzuki, T., Iwasaki, T., Uzawa, T., Hara, K., Nemoto, N., Kon, T., Ueki, T., Yamagishi, A. & Oshima, T. (2002). *Extremophiles*, **6**, 39–44.
- Trumpower, B. L. & Gennis, R. B. (1994). *Annu. Rev. Biochem.* **63**, 675–716.
- Uchiyama, T., Kounosu, A., Sato, T., Tanaka, N., Iwasaki, T. & Kumasaka, T. (2004). *Acta Cryst. D60*, 1487–1489.
- Vagin, A. & Teplyakov, A. (1997). *J. Appl. Cryst.* **30**, 1022–1025.
- Xiao, Z., Lavery, M. J., Ayhan, M., Scrofani, S. D. B., Wilce, M. C. J., Guss, J. M., Tregloan, P. A., George, G. N. & Wedd, A. G. (1998). *J. Am. Chem. Soc.* **120**, 4135–4150.